

# APPLICATION OF THE SPH METHOD TO SIMULATE COUPLED IONIC TRANSPORT AND ELECTRODEPOSITION IN LITHIUM BATTERIES

Madison Morey<sup>1</sup>, Emily Ryan<sup>1,2</sup>

<sup>1</sup>Division of Material Science and Engineering

<sup>2</sup>Department of Mechanical Engineering

Boston University

Boston, MA, USA

mmorey@bu.edu, ryanem@bu.edu

## I. INTRODUCTION

Long-duration energy storage and long-range electric vehicles are critical to meeting the demands of a more energy efficient future. Currently, the Lithium (Li)-ion battery (LIB) dominates the energy storage market. The LIB is composed of a negative electrode (anode) and a positive electrode (cathode) that determine the current and voltage outputs, an ion conducting electrolyte that transports Li cations ( $\text{Li}^+$ ) between electrodes, and a polymer separator that consists of small pores and prevents the direct contact of the anode and the cathode inhibiting short circuit of the battery [1]. While the LIB is generally stable during cycling, the graphite anode in the LIB has a low theoretical capacity ( $\sim 372 \text{ mA h g}^{-1}$ ) severely limiting the energy storage capabilities of this technology [2]. To combat these limitations, the Li metal battery (LMB) has emerged as a potential alternative. The LMB consists of the same major components as the LIB; however, instead of a graphite anode a Li-metal anode with a large theoretical capacity ( $\sim 3860 \text{ mA h g}^{-1}$ ) is used [2]. During operation the  $\text{Li}^+$  will react with electrons along anode-electrolyte interface and deposit as Li metal where it will be stored until discharge of the battery. While the LMB is a promising technology, its commercialization is hindered by an unstable anode-electrolyte interface and uncontrolled dendrite growth which cause decreased coulombic efficiency and safety concerns [3]. Therefore, a comprehensive understanding of the morphological evolution of electrodeposited Li is critical to its commercialization.

Additionally, the anode-electrolyte interface is difficult to study experimentally due to its embedded nature, thus computational methods can be used to resolve the interface allowing for the complex physics to be studied. Many different computational methods have been employed to model the phenomena at the anode-electrolyte interface including Monte Carlo methods [4], Diffusion Limited Aggregation (DLA) [5], and the Phase Field Method (PFM) [6]. While PFM has gained

traction in electrodeposition modeling, it struggles to accurately capture plating morphologies and often produces artificial symmetries. Therefore, to effectively model Li plating at the anode-electrolyte interface of LMBs, the Smoothed Particle Hydrodynamics (SPH) method has been adopted for this work due to its particle nature, making it well suited for simulating systems with moving and deforming boundaries without the need for front tracking methods [7]. Additionally, it can easily capture complex geometries such as dendrites.

The model uses a Nernst-Planck equation to track diffusion and migration within the electrolyte and is coupled with an extended Butler-Volmer equation to capture the reduction reaction of  $\text{Li}^+$  along the anode surface. The model can capture the electrodeposition process and accurately depicts Li plating morphologies based on experimental studies. Within this work, the model is used to study how the manufacturing and fabrication of varying components within the LMB including the electrode, electrolyte and separators influence Li plating morphology. Finally, the conditions in which the LMB is operated under will be evaluated and coupled with the manufacturing and fabrication to understand the interplay between operation and physical design of the anode-electrolyte interface.

## II. METHODS

In a binary electrolyte, salts are dissolved in a solvent where they disassociate into cations,  $\text{Li}^+$  for the application of LMBs, and anions remaining electrically neutral until the application of an applied current or voltage. Upon the application of the applied potential, anions will travel towards the cathode and  $\text{Li}^+$  will travel to the anode where they will be consumed. The consumption of cations at the anode-electrolyte interface leads to an imbalance in charge and a local potential,  $\phi$ , gradient as defined by the Electrostatic-Poisson equation

$$\nabla^2 \phi(\vec{r}_f, t) = -\frac{F(z_{\text{Li}^+} c_{\text{Li}^+}(\vec{r}_f, t) - z_A c_A(\vec{r}_f, t))}{\epsilon}, \vec{r}_f \in \Omega_f, t > 0 \quad (1)$$

where  $F$  is the Faraday constant,  $z$  is the ionic charge of the given species, cation ( $\text{Li}^+$ ) or anion ( $A$ ),  $C$  is the concentration of the ionic species,  $\epsilon$  is the dielectric constant,  $\vec{r}_f$  is the location of a given particle in the electrolyte domain,  $\Omega_f$ , and  $t$  is the time.

The Nernst-Planck equation governs the transport of ions and tracks the change in concentration of ions with respect to time,  $\partial C_i / \partial t$ ,

$$\frac{\partial C_i}{\partial t} = \nabla \cdot (D_i \nabla C_i) + \mu_i \nabla \cdot (C_i \nabla \phi), \vec{r}_f \in \Omega_f, t > 0. \quad (2)$$

The first term on the right-hand side of the equation tracks diffusion which is a response to a concentration gradient where  $D_i$  is the diffusion coefficient. The second term tracks migration where  $\mu_i$  is the mobility which defines how fast an ion moves with respect to an electric field. The subscript  $i$  denotes ion type (cation or anion) and  $\vec{r}_f$  is a specified location in the electrolyte,  $\Omega_f$ .

Upon reaching the anode-electrolyte interface, cations ( $\text{Li}^+$ ) react with electrons ( $e^-$ ) and deposit as Li metal (Li)



The reaction flux for a single hemispherical nucleate is governed by an extended Butler-Volmer equation

$$S_S(\vec{r}_s, t) = k^0 C_{\text{Li}^+, L}^{\alpha_c} C_{A, L}^{\alpha_a} \left[ \frac{C_{\text{Li}^+, L}(\vec{r}_s, t)}{C_{\text{Li}^+, L}} \exp\left(\alpha_a \left(\frac{F\eta}{RT} + \frac{2\gamma(\vec{r}_s) V_m}{r(\vec{r}_s, t) RT}\right)\right) - \exp\left(-\alpha_c \left(\frac{F\eta}{RT} + \frac{2\gamma(\vec{r}_s) V_m}{r(\vec{r}_s, t) RT}\right)\right) \right], \vec{r}_s \in \Gamma, t > 0 \quad (4)$$

where  $k^0$  is the reaction rate,  $\alpha_c$  and  $\alpha_a$  are the cathodic and anodic transfer coefficients, respectively,  $R$  is the ideal gas constant,  $T$  is the temperature,  $V_m$  is the molar volume,  $\gamma$  is the interfacial energy,  $C_{\text{Li}^+, L}$  and  $C_{A, L}$  are the cation and anion concentration in the bulk electrolyte, and  $r_s$  is a specified location along the reactive boundary,  $\Gamma$ . The overpotential,  $\eta$ , is defined by  $\eta = \phi_{\text{App}} - \phi(\vec{r}_f, t) - E^0$  where  $\phi_{\text{App}}$  is the applied potential and  $E^0$  is the standard electrode potential which is equal to zero in this system. The radius of a hemispherical nucleate is  $r$ , and the growth rate of the nucleate is governed by  $dr/dt = S_n(\vec{r}_s, t) * V_m$ .

Finally, the overall flux at the anode-electrolyte interface can be obtained by scaling the flux for a single nucleate (6) by the total number of nucleates in the system,  $S_S(\vec{r}_s, t) = S_n(\vec{r}_s, t) * n(\vec{r}_s, t)$ . The nucleation rate is defined by

$$\frac{dn(\vec{r}_s, t)}{dt} = \frac{3}{4} \left[ \frac{C_{\text{Li}^+, L}(\vec{r}_s, t) d V_m i_0 \eta F z_M^2}{e \gamma(\vec{r}_s) f(\theta)} \right] \left( \frac{\Delta G_c}{3 \pi k_B T} \right)^{1/2} \exp\left(-\frac{\Delta G_c}{k_B T}\right), \vec{r}_s \in \Gamma, t > 0 \quad (5)$$

where  $e$  is the elementary charge,  $k_B$  is the Boltzmann constant,  $d$  is the thickness of the electrolyte in the vicinity of the electrode ( $\sim 10$  angstroms),  $i_0$  is the exchange current density and  $f(\theta) = 1/2 - 3/4 \cos(\theta) - 1/4 \cos^3(\theta)$  is a scaling factor that

is a function of contact angle,  $\theta$ . The formation energy or the critical nucleus for an electrochemical system is determined by  $\Delta G_c = ze(\eta - \phi_{\text{App}})$ .

The reactive boundary condition for cations is given by

$$D_{\text{Li}^+} \nabla C_{\text{Li}^+}(\vec{r}_s, t) + \mu_{\text{Li}^+} C_{\text{Li}^+}(\vec{r}_s, t) \nabla \phi(\vec{r}_s, t) = S_S, \vec{r}_s \in \Gamma, t > 0 \quad (6)$$

and controls the electrodeposition process along the anode-electrolyte interface.

There is a zero-flux boundary condition for anions at the reactive boundary.

$$D_A(\vec{r}) \nabla C_A(\vec{r}_s, t) + \mu_A C_A(\vec{r}_s, t) = 0, \vec{r}_s \in \Gamma, t > 0 \quad (7)$$

The simulation domain consists of the anode, a layer adjacent to the anode known as the diffusion layer, where transport occurs, a reactive boundary that adapts to the newly formed plating morphologies, and a constant concentration region a distance  $L$  from the anode's surface to resemble the bulk electrolyte (Fig. 1). The governing equations are discretized using the SPH method and implemented into the open-source code base LAMMPS. The model has been verified and validated in previous work [8], [9], [10], [11], [12].

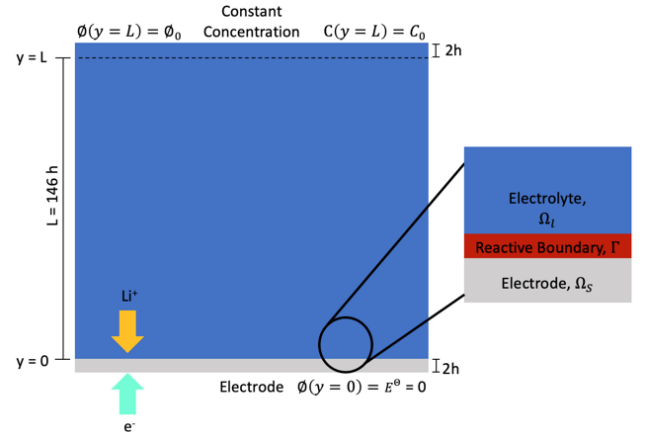


Figure 1. Schematic of the simulation domain including the anode surface (gray), the electrolyte (blue), and the reactive boundary (red) that will change shape and adapt to the growth of dendrites.

### III. RESULTS AND DISCUSSION

The formation and growth of Li dendrites is attributed to the high reactivity of Li metal and electrolyte, non-uniform transport of  $\text{Li}^+$  to the anode-electrolyte interface and uneven reactions. Further, balance between the manufacturing and fabrication of the physical system and the operational parameters that the system is driven by can either exasperate or mitigate problematic plating morphologies. In this work, the manufacturing and fabrication is studied from varying angles including the design of the electrolyte, separator, and electrode. Finally, alternative charging protocols such as pulse-plating (PP) are applied to the system to understand how electrodeposition can be controlled.

There are varying ways in which the anode-electrolyte interface can be manufactured to control Li deposition. In this work, we considered doping of the anode surface with impurity atoms through methods such as surface coatings and codeposition to tune the interfacial energy of the anode-electrolyte interface. Anode surfaces that possess higher interfacial energies resulted in suppressed dendrite growth in comparison to those with low interfacial energies. In addition to tuning the interfacial energy, Li plating on patterned anode surfaces was simulated and compared to that on a flat anode surface. It was found that at low rates of charging (0.1C), the Li deposition morphology was dense across the entire interface for both the flat surface and the patterned anode. However, as the charge rate increased (1C), the plating became more dendritic and large dendrites formed on the corners of the square hole patterns (Fig. 2a). Combining the patterned anodes with increased interfacial energy was also studied. Fig. 2b shows the Li plating morphology across the interface of a patterned surface when the interfacial energy is increased from  $1.715 \text{ J m}^{-2}$  to  $3.0 \text{ J m}^{-2}$ . When the interfacial energy is higher a denser Li deposition is observed, but there are still large dendrites forming at the corners of the hole, indicating that the interfacial energy alone, is not sufficient in controlling growth along the patterned interface at high charge rates.

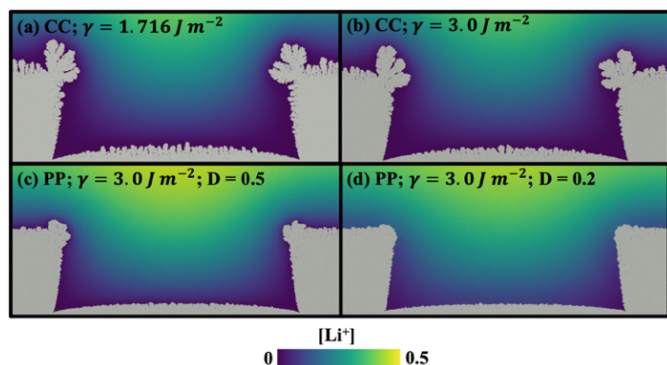


Figure 2. Model predicted Li plating morphology for (a) CC;  $\gamma=1.716 \text{ J m}^{-2}$  (b) CC;  $\gamma=3.0 \text{ J m}^{-2}$  (c) PP;  $\gamma=3.0 \text{ J m}^{-2}$ ;  $D=0.5$  and (d) PP;  $\gamma=3.0 \text{ J m}^{-2}$ ;  $D=0.2$ . The color scheme shows the  $\text{Li}^+$  concentration gradient and the solid particles are colored gray for visualization.

Utilizing alternative charging protocols, such as Pulse-Plating (PP) charging, can aid in stabilization of Li plating. PP methods utilize a quick charging potential, followed by a brief relaxation period to allow for  $\text{Li}^+$  to move into the interface before charging again. This protocol allows  $\text{Li}^+$  to be replenished at the anode-electrolyte interface leading to more uniform deposition. A PP protocol was applied to high interfacial energy, patterned anode (Fig. 2c and 2d) at two different duty cycles, which defines the ratio of charge to relaxation time. When a PP charging method is utilized, in comparison to the constant charging (CC), presented in Fig. 2a and 2b, significantly more uniform plating across the interface was present. When the duty cycle is 0.5, deposits still preferentially form at the corners of the hole patterns. However, decreasing the duty cycle to 0.2, which has the longest relaxation period, results in the most uniform deposition and no deposits forming at the corners of the hole patterns. While the improvement in Li plating morphology resulting from PP charging protocols is promising, the time it

takes for the system to reach a desired state of charge is significantly longer than the constant charging at the same charge rate, limiting its use for applications such as fast charging.

The SPH method was used in a novel way to develop a computational model that captures the morphological evolution of electroplated Li in LMBs. This work highlights how complex the Li plating process is and concludes that stabilizing the anode-electrolyte interface and suppressing dendrite growth is not straightforward and will require the optimization of the manufacturing/fabrication of the system and the operating conditions that drive deposition.

#### ACKNOWLEDGMENT

Financial support for this research was provided by the National Science Foundation through Award Nos. 2310353, 2034154, and 2216596, and the Graduate Research Fellowship Program through award No. 2234657.

#### REFERENCES

- [1] J. Yan, B. J. Xia, Y. C. Su, X. Z. Zhou, J. Zhang, and X. G. Zhang, "Phenomenologically modeling the formation and evolution of the solid electrolyte interface on the graphite electrode for lithium-ion batteries," *Electrochim Acta*, vol. 53, no. 24, pp. 7069–7078, Oct. 2008, doi: 10.1016/j.electacta.2008.05.032.
- [2] B. Liu, J. G. Zhang, and W. Xu, "Advancing Lithium Metal Batteries," May 16, 2018, *Cell Press*. doi: 10.1016/j.joule.2018.03.008.
- [3] X. Guan *et al.*, "Controlling Nucleation in Lithium Metal Anodes," *Small*, vol. 14, no. 37, Sep. 2018, doi: 10.1002/sml.201801423.
- [4] A. Aryanfar, D. Brooks, B. V. Merinov, W. A. Goddard, A. J. Colussi, and M. R. Hoffmann, "Dynamics of lithium dendrite growth and inhibition: Pulse charging experiments and monte carlo calculations," *Journal of Physical Chemistry Letters*, vol. 5, no. 10, pp. 1721–1726, May 2014, doi: 10.1021/jz500207a.
- [5] T. A. Witten and L. M. Sander, "Diffusion-Limited Aggregation, a Kinetic Critical Phenomenon," *Phys Rev Lett*, vol. 47, no. 19, pp. 1400–1403, Nov. 1981, doi: 10.1103/PhysRevLett.47.1400.
- [6] Y. Ren, Y. Zhou, and Y. Cao, "Inhibit of Lithium Dendrite Growth in Solid Composite Electrolyte by Phase-Field Modeling," *Journal of Physical Chemistry C*, vol. 124, no. 23, pp. 12195–12204, Jun. 2020, doi: 10.1021/acs.jpcc.0c01116.
- [7] J. J. Monaghan, "Smoothed particle hydrodynamics," Aug. 01, 2005. doi: 10.1088/0034-4885/68/8/R01.
- [8] A. Cannon, J. G. McDaniel, and E. Ryan, "Smoothed Particle Hydrodynamics Modeling of Electrodeposition and Dendritic Growth Under Migration- and Diffusion-Controlled Mass Transport," *Journal of Electrochemical Energy Conversion and Storage*, vol. 20, no. 4, Nov. 2023, doi: 10.1115/1.4056327.
- [9] J. Tan, A. Cannon, and E. Ryan, "Simulating dendrite growth in lithium batteries under cycling conditions," *J Power Sources*, vol. 463, Jul. 2020, doi: 10.1016/j.jpowsour.2020.228187.
- [10] M. Morey, J. Loftus, A. Cannon, and E. Ryan, "Interfacial studies on the effects of patterned anodes for guided lithium deposition in lithium metal batteries," *Journal of Chemical Physics*, vol. 156, no. 1, Jan. 2022, doi: 10.1063/5.0073358.
- [11] T. Melsheimer, M. Morey, A. Cannon, and E. Ryan, "Modeling the effects of pulse plating on dendrite growth in lithium metal batteries," *Electrochim Acta*, vol. 433, Nov. 2022, doi: 10.1016/j.electacta.2022.141227.
- [12] M. Morey, G. Nagaro, A. Halder, S. Sharifzadeh, and E. Ryan, "A framework for nucleation in electrochemical systems and the effect of surface energy on dendrite growth," *J Energy Storage*, vol. 92, Jul. 2024, doi: 10.1016/j.est.2024.112144.